R. Casasola, J.M. Pérez, M. Romero, Glass forming ability and thermal stability of F-phlogopite based glasses. Journal of Thermal Analysis and Calorimetry 121 (2015), 843-853; doi: 10.1007/s10973-015-4524-1

Glass forming ability and thermal stability of F-phlogopite based glasses

R. Casasola, J.M. Pérez, M. Romero*

Group of Glass and Ceramic Materials, Instituto de Ciencias de la Construcción Eduardo Torroja, CSIC. C/ Serrano Galvache 4. 28033 Madrid. Spain.

* Corresponding author, Tel.: +34 91 302 04 40; Fax: + 34 91 302 07 00.
e-mail address: mromero@ietcc.csic.es

Abstract

This paper presents the results of a study that analyses the effect of fluorine content on glass forming ability (GFA), glass stability (GS) and preferred crystallisation mechanism for a series of glasses in the SiO_2-Al_2O_3-MgO-K_2O-F system. Three glass compositions, with fluorine contents ranging from 4.50 to 5.70 wt. %, were investigated by differential scanning calorimetry (DSC). The GS was established by estimating different parameters derived from characteristic temperatures of non-isothermal DSC curves, namely, the working range (ΔT_{TS}), reduced glass transition temperature (T_{gr}), Weinberg (K_w), Hrubÿ (K_H) and Lu-Liu (K_{LL}) parameters. The prevalent crystallisation mechanism for each glass was assessed by determining the dissimilarity in crystallisation temperature (ΔT_p) between fine (<63µm powder) and coarse glass samples. The estimation of glass forming ability (GFA) was based on the critical cooling rate (q_c), which is determined from the Weinberg, Hrubÿ and Lu-Liu parameters. The results point out that the compositions of these glasses result in melts with a high tendency to crystallize during cooling (q_c > 120°C/min) and obtaining amorphous glasses is only possible by fast cooling of the melt. In a subsequent thermal treatment, a volume crystallization mechanism will be prevalent in the process of devitrification of these F-phlogopite based glasses. Nevertheless, the increasing on the fluorine content in the glass composition leads to a variation in the location of the first developed crystals from the internal volume of the glass particle to surface sites. The results established by DSC analyses are verified by the results obtained from field emission scanning electron microscopy (FESEM) and X-ray diffraction (XRD).

Keywords: F-phlogopite; DSC; Hrubrÿ, Weinberg; Lu-Liu; glass-forming ability; crystallisation mechanism

1. Introduction

Fluorphlogopite (hereinafter, F-phlogopite) is a phyllosilicate with empirical formula $KMg_3(Si_3Al)O_{10}F_2$ showing lamellar structure of trioctahedral mica. This type of mica shows a *t-o-t* structure in which the sheets are composed of $[SiO_4]^{4-}$ units joined together to form hexagons, so that each units sharing three oxygen ions with and adjacent tetrahedra. When these type *t-o-t* stacks are electrically neutral they form structurally stable units connected together by Van der Waals bonds. The weakness of these links favours the exfoliation of micas. However, if a Si^{4+} atom is replaced by an Al^{3+} ion, a negative charge is generated, which is able to join monovalent cations in regular coordination 12 between *t-o-t* stacks. As a result of these 'sandwich'-cation-'sandwich' links, the structure of this type of mica is kept more firmly bonded, decreasing its easiness of sliding while increasing its hardness. Micas with cations between layers generally form tabular crystals with well-developed basal planes and rhomboidal or hexagonal shape, characterized by a {001} perfect basal cleavage [1].

Glass-ceramics containing F-phlogopite have been studied taking into account their properties and potential applications, which are dependent on their highly anisotropic crystallography [2,3]. One of the attributes that have resulted in highest number of publications is their machinability [4-6]. Compared to other ceramics, glass-ceramics containing F-phlogopite phase can be machined by using conventional cutting tools. This feature is due to its microstructure characterized by cross-linked mica flakes immersed in a residual glass matrix. The cracks initiated during cutting are deflected parallel to the basal plane of mica [7,8], allowing the gradual removal of particles whereas the workpiece is being machined and without damaging the rest of the sample [9]. The machinability of these glass-ceramics depends on the amount of crystalline phase developed, of the dimensions of phlogopite crystals and the extent of crosslinking between them. In this sense, KhatibZadeha et al. [10] studied the machinability of F-phlogopite glass-ceramics obtained by both traditional (from bulk pieces) and sintering (from granulated glass) processing route. The results showed that the material obtained by the sintering method exhibited better machinability and mechanical properties than that prepared from a bulk piece as a consequence of the greater percentage and the smaller size of F-phlogopite crystals developed in sintered pieces.

Glass-ceramics containing F-phlogopite has also been studied from the point of view of its application as biomaterial. Materials known as bioceramics can be classified into two groups: biocompatible materials, when they present a neutral behaviour, producing no reaction with the body tissues and fluids; and bioactive materials, when they have the ability to react with its environment resulting in bone tissues. F-phlogopite phase is not bioactive by itself but it

exhibits better machinability and mechanical properties than other bioactive glass-ceramic whose main crystalline phase is the F-apatite ($Ca_5(PO_4)_3F$). In order to improve the properties of bioceramics, several researches on sintering and crystallization frit compositions based on F-phlogopite and F-apatite [11,12] has been conducted.

F-phlogopite glass-ceramics have been also applied as Nicalon^{TM} fibre reinforcement. These fibres are usually reinforced with lithium or calcium aluminosilicates and they possess an interface enriched in carbon, formed in situ during the process of consolidation of the material. This thin layer allows deflection of the cracks, providing greater resistance to the fibres. The structural and mechanistic similarities between graphite and mica crystals, together with the oxidation resistance of the latter led to Chyung and Dawes [13] to study the application of F-phlogopite glass-ceramics as Nicalon^{TM} fibre reinforcement. They concluded that as the fibres are subjected to high temperatures in oxidizing atmospheres, boundaries containing K-F-phlogopite were more resistant than the original carbon-rich interfaces.

F-phlogopite has been also introduced as crystalline phase in glass-ceramic glazes [14]. Romero et al. [15] highlighted that the development of preferential crystal orientation together with a high interlocking of mica crystals lead to the development of glazes showing improved mechanical properties. Thus, the value of fracture toughness of mica glass-ceramic glaze is 2.3 times greater than that of the amorphous base glaze.

Therefore, F-phlogopite glass-ceramics have been shown to feature favourable properties [16]. However, little literature on the capability of F-phlogopite based melts to develop amorphous glasses and on the progress of crystals at the earliest stages of devitrification of F-phlogopite glasses has been reported.

Differential thermal analysis (DTA) and differential scanning calorimetry (DSC) techniques are normally used to know the main parameters required for understanding glass crystallisation behaviour [17-21]. The aim of the present paper is to investigate by DSC the effect of fluorine content on glass forming ability, glass stability and the crystallisation mechanism of a series of glasses that are based on F-phlogopite composition (SiO_2-Al_2O_3-MgO-K_2O-F system). This research is part of a larger study that explores the crystallisation process and final properties of the resulting glass-ceramic materials, in an effort to discover novel applications in the field of glass-ceramic glazes for ceramic tiles.

2. Experimental

A glass in the SiO_2-Al_2O_3-MgO-K_2O-F system with the stoechiometric composition of fluor-flogopite, $KMg_3(Si_3AlO_{10})F_2$ and hereafter designated as FE glass, was formulated based on a reagent grade Al_2O_3, $(MgCO_3)_4Mg(OH)_2{\cdot}5H_2O$, K_2CO_3 and MgF_2. Moreover, silica sand (El Espirdo, Spain) was used as silica source. It was a high purity sand with a 98 wt.% of SiO_2 and low content of chromophore oxides, such as Fe_2O_3 (0.31 wt.%) or TiO_2 (0.57 wt. %). Based on the composition of FE, two additional glass compositions were formulated. They contained 10 and 12 wt. % of fluorine and were designated as F10 and F12, respectively.

The raw materials mixtures were homogenised in a planetary ball mill (TURBULA) for 15 min. The batches were placed in alumina-silica crucibles and then melted at 1450ºC for 2 h in an electric furnace. From the different compositions, it was attempted to achieve glasses in both frit and bulk form. Frit glasses were obtained by pouring the low-viscosity melts into cool water. An effort to get monolithic glass samples were made by casting the melt onto brass moulds.

The chemical composition of the resulting glasses was determined by X-ray fluorescence (XRF) using a BRUCKER S8 Tiger spectrometer. The analysis was performed on pressed pellets of powder glass samples. Powder glass samples were obtained by grinding the glass frits and subsequent sieving up to <63 μm. The evaluation of the amorphous nature of the glass after melting was performed by X-ray diffraction (XRD) using BRUKER D8 Advance equipment with Ni-filtered Cu Kα radiation operating at 30 mA and 40 kV. Data were recorded in the 5–60° 2θ range (step size 0.019732º and 0.5 s counting time for each step). In those cases where the X-ray pattern showed evidences of glass devitrification, the crystalline phases were identified by comparison with JCPDS Cards 16-0352 (F-phlogopite, $KMg_3(Si_3Al)O_{10}F_2$), 85-1364 (forsterite, Mg_2SiO_4) and 14-0010 (chondrodite, $Mg_5F_2(SiO_4)_2$).

The glass stability (GS) study was conducted by DSC on both fine (<63 μm powder) and coarse (~ 3 x 3 x 4 mm fragment) samples. DSC runs were performed in a SETARAM Labsys Thermal Analyser. The samples were heated from room temperature to 1400ºC at a heating rate of 50ºC·min^{-1} under flowing air. Samples of ~ 40 mg were placed in platinum crucibles and calcined Al_2O_3 was used as reference material. All the DSC curves were normalised with respect to the sample mass. The temperature precision given by the equipment is ± 0.1 ºC. Each measurement was reproduced three times in order to estimate experimental errors. To confirm the effect of fluorine on the preferential crystallisation mechanism (surface or volume), samples of glass frit of the different compositions were subjected to a heat treatment at 850°C for 10 minutes in order to prompt crystal growth. The microstructure of the resulting glass-ceramic

materials was observed by field emission scanning electron microscopy (FESEM) with a HITACHI S-4800P microscope using an acceleration voltage of 20 kV. Glass-ceramic particles were polished to a 1 μm finish using diamond pastes after initially grinding with SiC powder. The samples were subsequently etched for 10 s in a solution of 5% HF, ultrasonically washwith distilled water and ethylic alcohol, dried and coated with Au-Pd in a Balzers SCD 050 sputter.

Typically, when a glass undergoes a thermal treatment, devitrification arises as a consequence of the energy reduction that occurs when the structurally amorphous phase (glass) is transformed in a stable solid phase with a regular ordered geometry [22]. Glass stability (GS) symbolizes the resistance of a glass to crystallisation on heating. The GS of each glass composition was evaluated by means of different parameters calculated from the characteristic temperatures obtained from DSC curves; namely, the glass transition temperature (T_g), onset and peak crystallisation temperatures (T_x and T_p, respectively), and melting temperature (T_m), which is the temperature at the minimum of the endothermic peak.

The devitrification of a glass can progress by means of two mechanisms: volume or bulk crystallisation and surface crystallisation. In volume crystallisation, crystals are homogeneously and randomly distributed throughout the entire volume of the glass. Conversely, in surface crystallisation, crystals develop at the glass surface and then grow into the glass volume. The Thakur and Thiagarajan method [22] was used to establish the predominant crystallisation mechanism for each glass composition by determining the crystallisation temperature difference between fine and coarse glass samples, ΔT_p, as follows:

$$\Delta T_p = T_{p\,(powder)} - T_{p\,(fragment)} \quad (1)$$

- Working range ΔT_{TS} [23],

$$\Delta T_{TS} = T_x - T_g \quad (2)$$

- Reduced glass transition temperature T_{gr} [24],

$$T_{gr} = \frac{T_g}{T_m} \quad (3)$$

- Weinberg (K_W) [25], Hrubÿ (K_H) [26] and Lu-Liu (K_{LL}) [27,28] parameters:

$$K_W = \frac{T_x - T_g}{T_m} \quad (4)$$

$$K_H = \frac{T_x - T_g}{T_m - T_x} \quad (5)$$

$$K_{LL} = \frac{T_x}{T_g + T_m} \quad (6)$$

Glass-forming ability (GFA) is defined as the ability of a melt to develop a glass during cooling. It can be estimated by the critical cooling rate q_c, which is the lowest rate, from melting to T_g, for preventing crystallisation. This critical cooling rate can be determined from the Weinberg (q_w), Hrubÿ (q_H) and Lu-Liu (q_{LL}) parameters by the following equations:

$$log_{10}q_W = 4.44 - 21.4 \cdot K_W \quad (7)$$

$$log_{10}q_H = 3.17 - 2.26 \cdot K_H \quad (8)$$

$$log_{10}q_{LL} = 17.7 - 34.6 \cdot K_{LL} \quad (9)$$

In this case, T_p instead of T_x has been used to determine the K_W, K_H and K_{LL} [29,30].

The effect of fluorine on the GFA of these glasses has been confirmed by in situ DSC examinations that reproduce the melting schedule applied in getting the glasses. Therefore, a mixture of raw materials of each glass composition was heated in the DSC apparatus to a maximum of 1450ºC with a heating rate of 50 ºC/min and held at the melting temperature for 30 min. Then, the sample was cooled to room temperature at 50ºC/min (higher cooling rates are unachievable by the equipment) and right away subjected to a new heating step at 50ºC/min to 1450ºC. Hence, the GFA of the melts can be evaluated from the DSC curves recorded during the first cooling step and the GS of the glasses from the DSC curves recorded during the second heating ramp. To identify the crystalline phases developed on cooling, the mixture of raw materials of each glass composition was melted in an electric furnace under the same conditions used for "in situ" DSC runs. To facilitate the development of crystalline phases, the melts were cooling at 50°C/min from 1450ºC to the temperature of their corresponding exothermic effect showed in the in situ DSC curves recorded during the first cooling step and then held for 30 min. After that, the samples were removed from the oven and cooled in air.

3. Results

After the melting of raw materials batches, the melts were cooled by pouring the melt both on brass mould and on cool water in order to obtain glass in bulk and frit form, respectively. Melts cooled on water leads to homogeneous, transparent and free of defect frits. In contrast, bulk glasses showed an inhomogeneous appearance with opalescent regions. As an example, Figure 1 shows the XRD diffractograms of F10 glass obtained in both frit and bulk form. The diffractogram recorded from the frit sample shows a broad diffraction halo in the 2θ = 20-40° range, which is characteristic of amorphous materials. In contrast, the pattern corresponding to the bulk glass shows defined diffraction peaks indicating the development of crystalline phases on melt cooling.

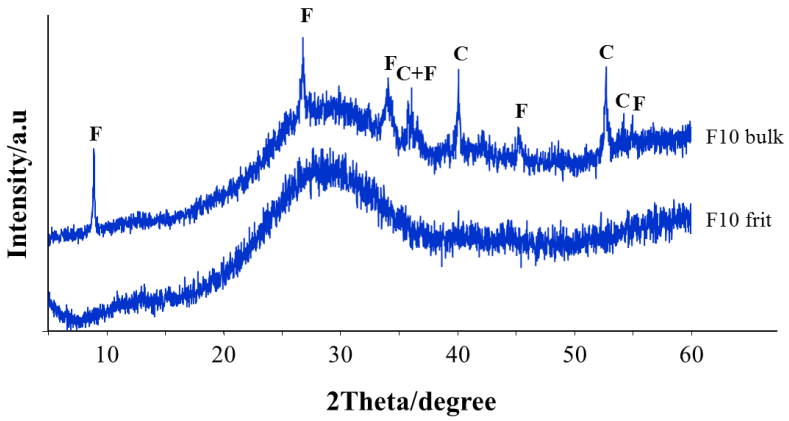

Figure 1. XRD of frit and bulk F10 glass samples. **F**= F-phlogopite $KMg_3(Si_3AlO_{10})F_2$; **C**=chondrodite $(Mg_5F_2(SiO_4)_2$.

Table 1 collects the experimental chemical composition of the investigated glasses determined by X-ray fluorescence. For a better discussion of the compositional changes taking place during the melting process, the theoretical composition of the glasses is also included.

Table 1. Theoretical and experimental (XRF) chemical composition (wt. %) of the investigated glasses.

		SiO_2	Al_2O_3	MgO	K_2O	F_2
FE	Theoretical	41.24	11.63	27.66	10.77	8.69
	Experimental	44.09	16.85	24.85	9.72	4.49
F10	Theoretical	40.65	11.47	27.26	10.62	10.00
	Experimental	44.05	17.04	24.32	9.68	4.91
F12	Theoretical	39.75	11.21	26.65	10.38	12.00
	Experimental	44.28	17.47	24.47	8.09	5.69

Figure 2 presents the DSC curves of F-phlogopite glasses recorded from samples with two different particle sizes, i.e., fine (<63 μm powder) and coarse (~ 3 x 3 x 4 mm fragment) samples. At around 660ºC, the thermograms show the distinctive endothermic fall in the baseline corresponding to the glass transition temperature (T_g). At higher temperatures, the DSC curves show two exothermic peaks (T_{p1} and T_{p2}) indicating that subsequent heat treatments of these glasses could lead to the devitrification of at least two different crystalline phases in separated thermal intervals. After these exothermic crystallization processes, the curves exhibit two endothermic peaks (T_{m1} and T_{m2}) corresponding to the processes of dissolution of previously formed crystalline phases. This thermal behaviour is observed in all the DSC curves

except that corresponding to F12 fragment, in which both the crystallization and the liquid phases formation processes are revealed by a single exo- or endothermic peak.

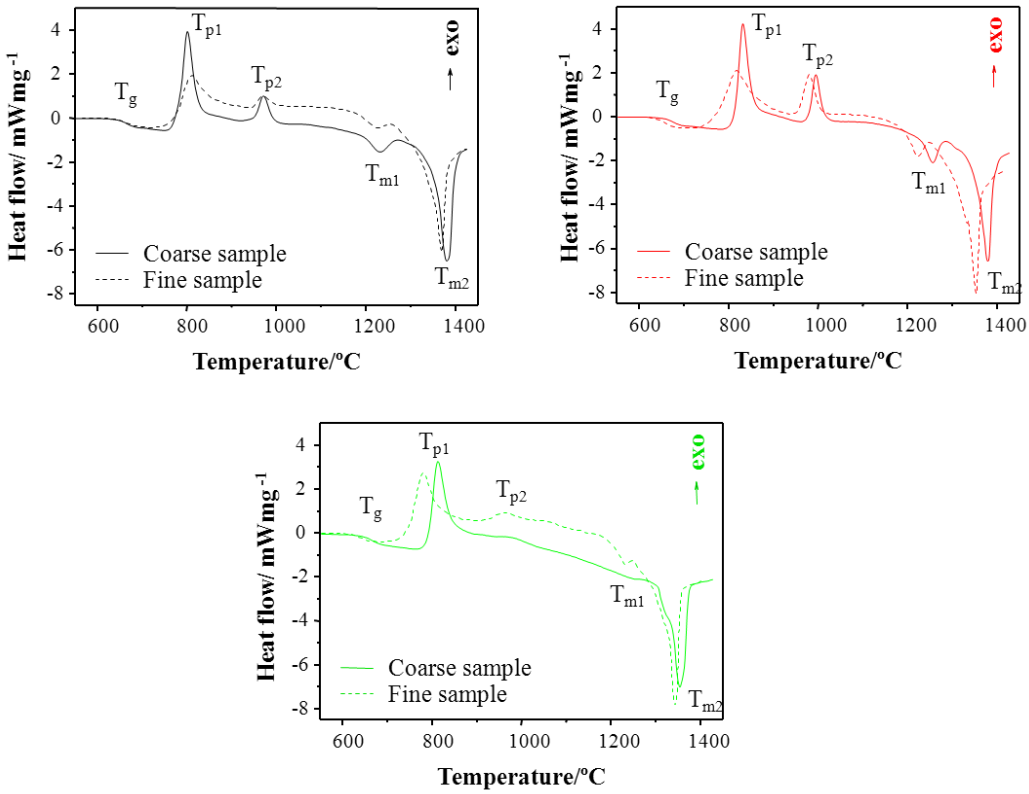

Figure 2. DSC thermograms from fine (<63 μm) and coarse glass samples at a heating rate of 50 ºC·min^{-1}.

Table 2 lists the values of the characteristic temperatures derived from the DSC curves.

Table 2. Characteristics temperatures derived from DSC curves for F-phlogopite based glasses. The errors in the characteristics temperatures are approximately ±2-3ºC.

Glass	Particle size	Tg	Tx1	Tp1	Tp2	Tm1	Tm2
FE	Coarse	663	748	801	970	1230	1380
	Fine < 63 μm		723	810	970	1225	1370
F10	Coarse	663	784	828	991	1253	1375
	Fine < 63 μm		733	828	990	1232	1362
F12	Coarse	659	765	810	-	-	1359
	Fine < 63 μm		709	794	977	1246	1361

The effect of fluorine on the crystallisation mechanism of these glasses has been evaluated from the values of ΔT_p, T_{gr} and ΔT_{TS} parameters. Figure 3 shows the evolution of ΔT_p, as determined from Equation 1.

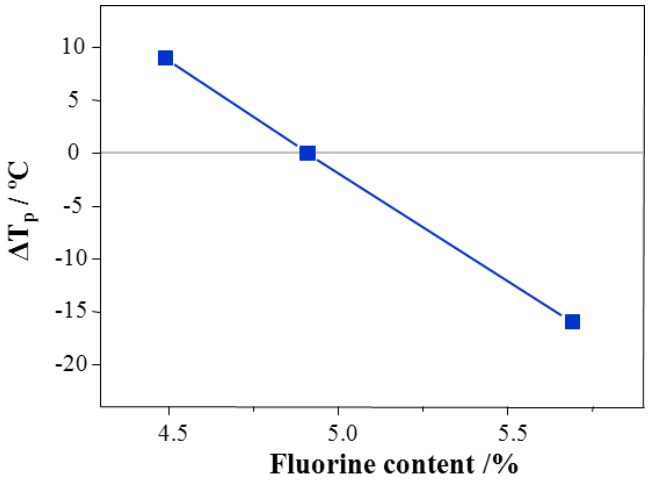

Figure 3. Evolution of ΔT_p with fluorine content for each glass composition (The lines are drawn to guide eyes). The errors in ΔT_p are approximately ±2-3º C.

Figure 4 illustrates the values of T_{gr} for the different glass compositions in both coarse and fine (<63µm) samples. T_{gr} is related to the critical cooling rate [31], thus, the lower the value of T_{gr}, the higher is the required q_c to avoid crystallisation from the melt during cooling. The lines depicted in Fig. 4 establish the gap between surface and bulk crystallisation [32-34].

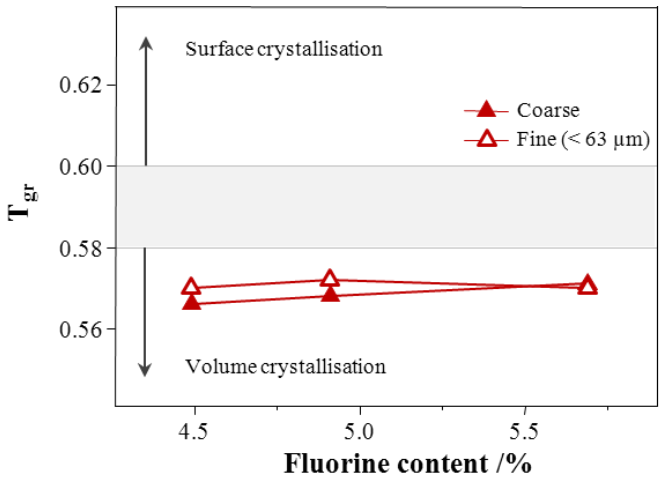

Figure 4. Values of T_{gr} for the different glass compositions in both coarse and fine (<63µm). The lines establish the gap between surface (T_{gr} > 0.58–0.60) and bulk (T_{gr} < 0.58–0.60) crystallisation. The errors in T_{gr} are approximately ±2-3º C.

To verify the preferred crystallization mechanism (surface or volume) by which the crystallization of these F-phlogopite based glasses takes place, samples of glass frit of the different compositions were subjected to a heat treatment at 850°C for 10 minutes in order to promoting the beginning of crystal growth. Figure 5 shows the microstructure observed by FESEM in the heat-treated samples.

The evaluation of the thermal stability of each glass was achieved by measuring its working range.

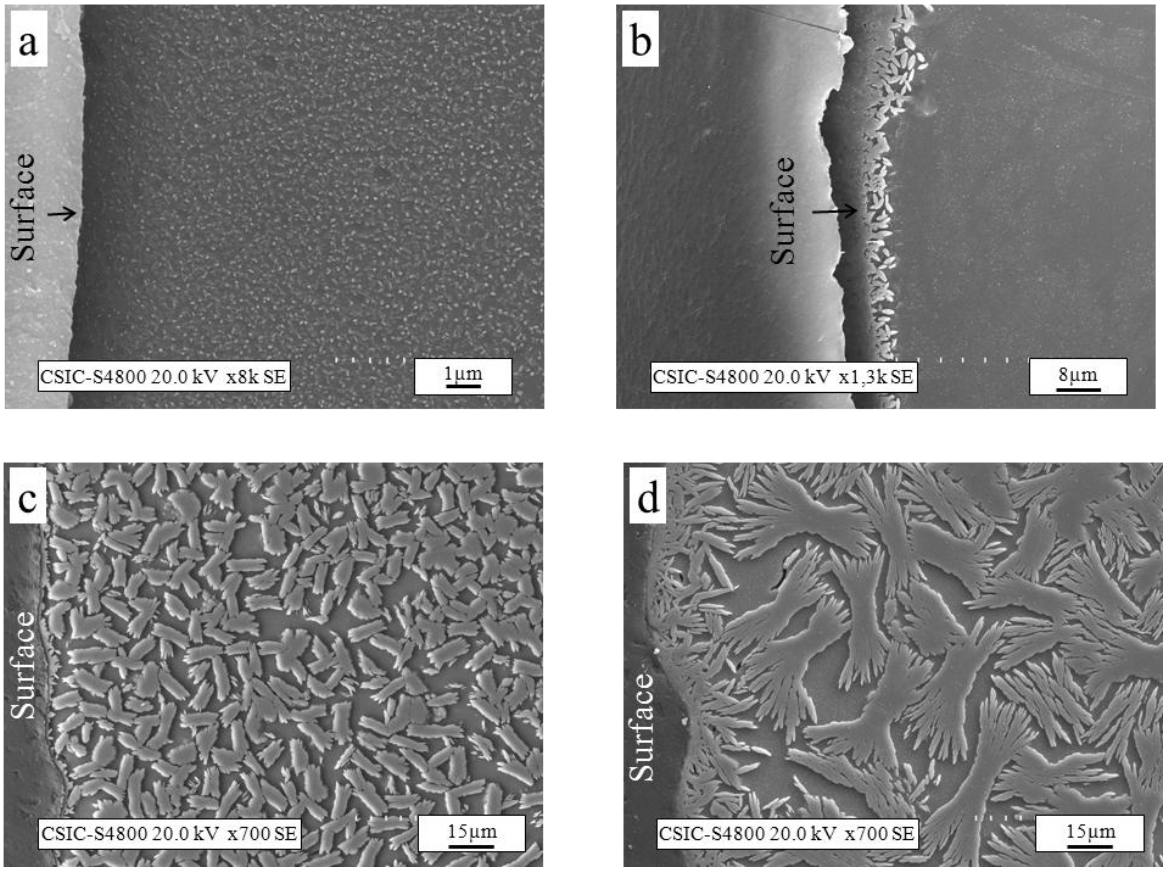

Figure 5. FESEM micrographs of heat-treated samples at the early stages of the crystallisation process. a) FE treated at 850ºC for 10 min; b) FE treated at 850ºC for 10+10 min; c) F10 treated at 850ºC for 10 min; d) F12 treated at 850ºC for 10 min.

Figure 6 depicts the evolution of ΔT_{TS} with fluorine content for both coarse and fine glass samples. The lower the value of ΔT_{TS}, the lower is the thermal stability of the glass and the easier it is to develop crystalline phases during heating [35]. The ability of these glasses to devitrify during the heating process has also been evaluated by K_H, K_W and K_{LL} parameters, so

that, the higher the value of these parameters, the more difficult is to obtain a crystallised material.

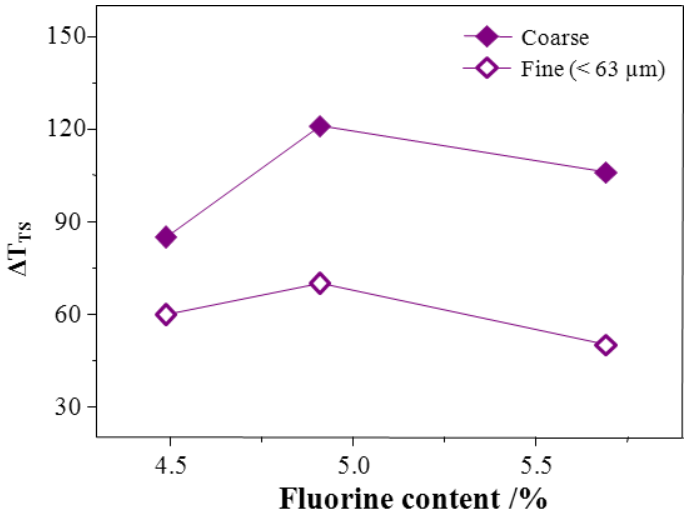

Figure 6. Evolution of ΔT_{TS} with fluorine content for both coarse and fine glass samples. The errors in ΔT_{TS} are approximately ±2-3º C.

Figure 7 illustrates the evolution these parameters with fluorine content. The glass forming ability (GFA) of these glasses has been assessed by means of the critical cooling rate, which can be determine from the K_H, K_W and K_{LL} parameters.

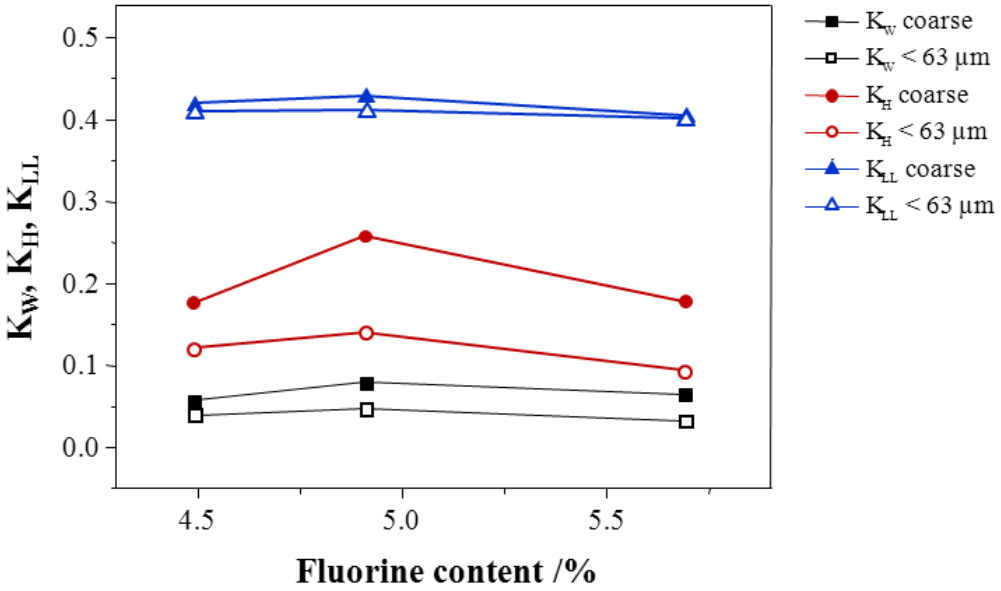

Figure 7. Hrüby (K_H), Weinberg (K_W) and Lu-Liu (K_{LL}) parameters for both coarse and fine glass samples.

Table 3 collects the q_c values calculated from the different GS parameters. The effect of fluorine on the GFA of these glasses has been also verified by in-situ DSC scans that simulate the melting cycle used in the preparation of the glasses.

Table 3. Critical cooling rates for F-phlogopite based glasses determined from Weinberg (q_W), Hrubÿ (q_H) and Lu-Liu (q_{LL}) parameters.

	q_W /ºC min^{-1}	q_H /ºC min^{-1}	q_{LL} /ºC min^{-1}
FE	219	234	202
F10	124	177	124
F12	345	313	434

Figure 8 shows the in-situ DSC curves recorded from the different raw materials mixtures. GFA of the melts can be evaluated from the scans registered during the first cooling step (Fig. 8a) and the GS of the glasses from the DSC curves recorded during the second heating ramp (Fig. 8b). The nature of the crystalline phases developed on cooling was ascertained by holding the melts at the temperature of their corresponding exothermic effect in Fig. 8a, in order to induce the growth of crystalline phases. After that, samples were removed from the oven and cooled in air. Figures 9 and 10 show the XRD patterns of the resulting materials.

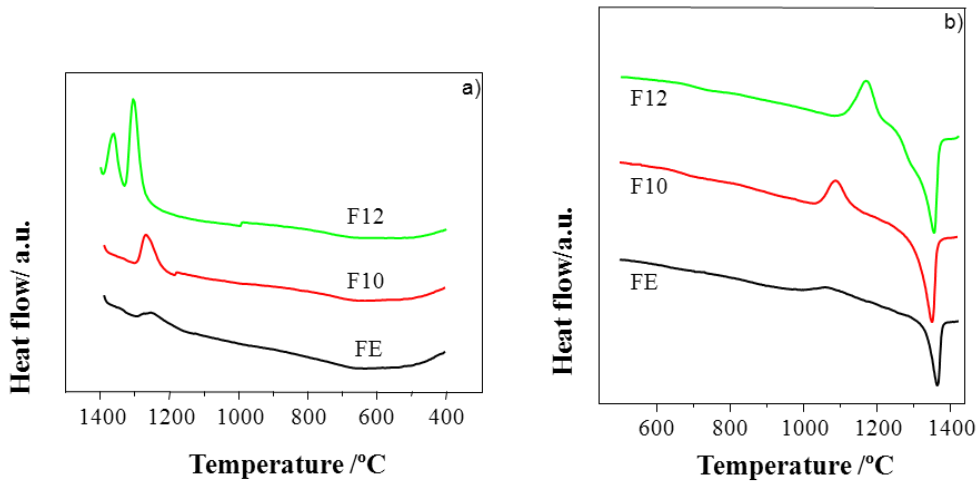

Figure 8. DSC curves from a mixture of raw materials of each glass composition, which were heated in the DSC equipment to 1450ºC and held for 30 min. Subsequently, the samples were cooled to room temperature at 50ºC/min (Fig. 8a) and immediately subjected to a new heating ramp at 50ºC/min to 1450ºC (Fig. 8b).

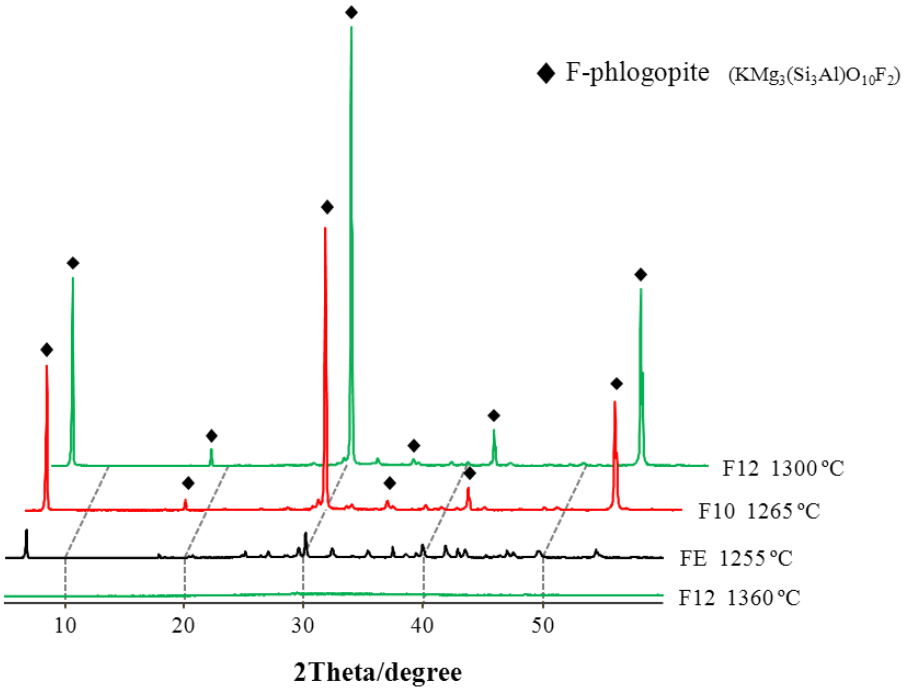

Figure 9. XRD patterns of the materials resulted after stopping the melt cooling for 30 min at the temperature of their corresponding exothermic effect in Fig. 8a.

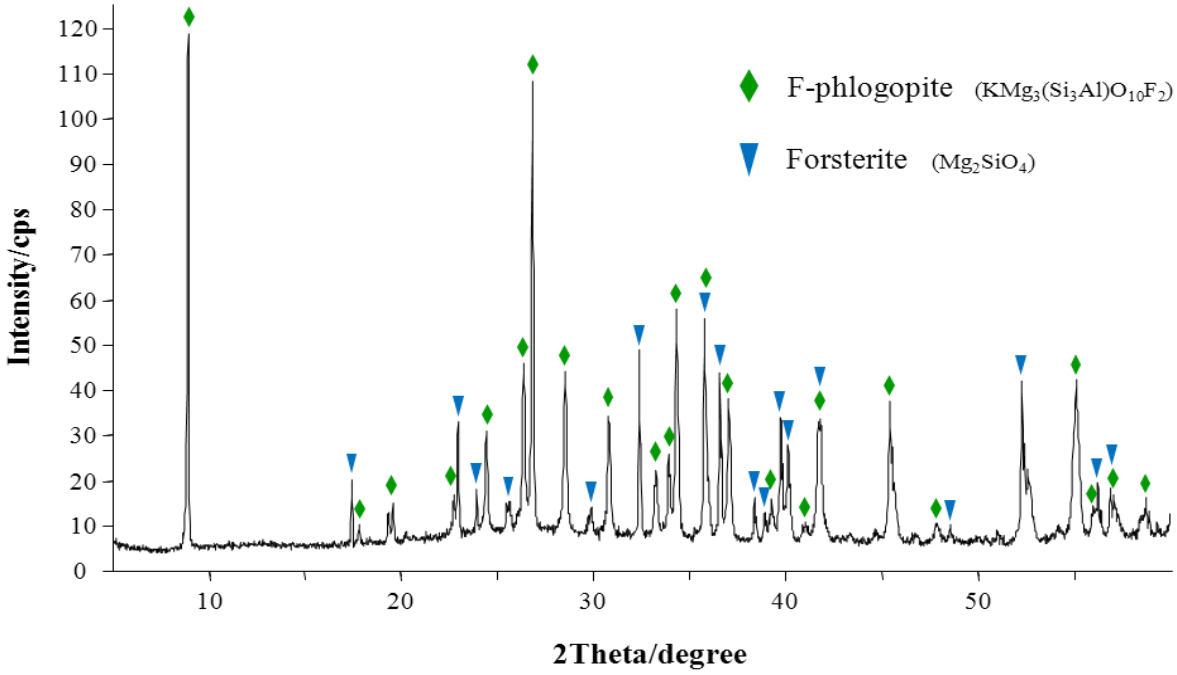

Figure 10. XRD pattern of the material resulted after stopping the FE melt cooling at 1255ºC for 30 min.

4. Discussion

Fig. 1 indicates that the compositions studied lead to melt showing high tendency to develop crystalline phases on cooling, so that it has only been possible to obtain totally amorphous materials through a fast cooling of the melt by casting in water. In bulk samples, XRD analysis shows the existence of diffraction peaks corresponding to F-phlogopite ($KMg_3(Si_3AlO_{10})F_2$, PDF 16-0352) and chondrodite ($Mg_5F_2(SiO_4)_2$, PDF 14-0010) phases. Because of this fact, the study described hereafter was performed only with samples of shaped glass frit.

Table 1 shows that during the melting process the molten glass is enriched in silica and alumina, so that the contents of these oxides in the cooled glasses are higher than expected theoretically. This increase is due to corrosion of the melt against the walls of the refractory crucibles (silico-alumina) used in the melting of raw materials mixtures [36]. At 1450ºC, the melt composition corrodes the inner surface of the crucibles, thus incorporating its components to the final glass composition. The higher the initial fluorine content in the mixture, the greater the percentage of silica and alumina incorporated in the melt, while the greater the proportion in which the fluorine content decreases in the glass composition. The increase in the relative proportions of these components (SiO_2, Al_2O_3) results in lowering the content of the other constituents (MgO, K_2O and F_2). Fluorine is the element whose percentage is reduced to a greater extent (~ 48-53%), which suggests that there must be some other factor contributing to this effect. In this sense, Likitvanichkul et al. [37] in a study of glasses in the CaO-Al_2O_3-SiO_2-M_2O-F_2 system showed that the loss of fluoride is mainly due to volatilization as SiF_4 and MF during the melting process. This finding has been also highlighted in a previous work on glass stability and crystallisation mechanism for fluoride glasses in the SiO_2–CaO–K_2O–F system [38].

Considering the DSC curves recorded from both coarse and fine glass samples (Fig. 2), in all cases the peak associated to the first exothermic effect (T_{p1}) is more intense than the second (T_{p2}), which suggests that the crystalline phase developed in the first crystallization stage would be predominant in relation to that formed as results of the second crystallization step at higher temperature. With regard to the endothermic effects associated with the formation of liquid phases, in this case the second endothermic (T_{f2}) shows higher intensity than the first (T_{f1}). In the DSC curve for F12 frit fragment where the T_{p2} exothermic is not detected, neither the T_{f1} endothermic effect is displayed, indicating that both peaks are related so that the crystalline phases that develop in the second exothermic process (T_{p2}) is dissolved in the first

endothermic(T_{f1}). Similarly, the phases that crystallize in the first exothermic (T_{p1}) is dissolved at the temperature of the second endothermic (T_{f2}).

The glass transition temperature (T_g) is an intrinsic property of the glass and hence, for a given glass composition the T_g value is constant regardless of the particle size of the sample. In this glasses fluorine does not exerts a clear fluidising effect, since as seen in Table 2, increasing the fluorine content in the glass composition does not result in a significant decrease of T_g. Similarly, increasing the fluorine content in the glass composition does not influence significantly on the mechanism of preferential crystallization of these glasses, since no significant variation in the characteristic temperatures are detected. This results contrasts with previous studies that has highlighted the fluidising action of F^- ions (T_g and T_x decreases with increasing fluorine content) in glasses in the SiO_2–CaO–K_2O–F [38], SiO_2-Al_2O_3-MgO-F [39] and SiO_2-Al_2O_3-MgO-BaO-F [40] systems. It may come from the fact that the difference in real fluorine is over 1%wt and so; the tendency showed in T_g can be insufficient to set a proper comparison. The fluidising effect of fluorine in glasses of different compositional systems has been also reported by different authors [41-43].

In the process of devitrification of these glasses concur two crystallization mechanisms (surface and volume) as DSC curves of glass samples with different particle sizes have well-defined exothermic peaks. Noting the first exothermic peak (T_{p1}), in all glasses the thermograms recorded from fragment samples exhibit a more distinct peak (narrower and with higher intensity) than that corresponding to fine (<63μm) samples. This result indicates that in a subsequent heat treatment, coarse samples will reach a crystalline degree more extensive and thus, the volume crystallization mechanism will be dominant in all glasses of this series. However, as the percentage of fluorine in the glass composition increases, a variation in both the relative position and height of T_{p1} from powder samples ($T_{p1\,p}$, $h_{1\,p}$) and fragment ($T_{p1\,c}$, $h_{1\,c}$) is clearly observed; so that $T_{p1\,c} < T_{p1\,p}$ in FE glass with the lower concentrations of fluorine (4.49%), $T_{p1\,c} \approx T_{p1\,p}$ in F10 glass and eventually $T_{p1\,c} > T_{p1\,p}$ in F12 glass with the higher fluorine content (5.69%). Regarding the peak height, it is observed that increasing the fluorine slightly reduces the peak intensity in the DSC curve recorded from the glass fragment sample, while in the powder sample (<63μm) the high of the first exothermic peak increases. Hence, the $h_{1\,c}/h_{1\,p}$ ratio decreases from a value of 1.9 in the FE glass up to 1.3 in F12.

This result indicates that increasing the fluorine content in these glasses enhances the formation of crystals on the surface of the glass particles. This effect is more clearly seen in Fig. 3, which depicts the variation of ΔT_p with the percentage of fluorine in the glass composition. It

is clear that ΔT_p decreases from $\Delta T_p = 9$ in the glass FE to $\Delta T_p = -16$ in the glass F12 as the fluorine content increases. These findings suggest a change in the spatial position at which the crystal nuclei are developed in the early stages of the crystallization process. Thus, the devitrification of the FE glass with $\Delta T_p > 0$ will start with the growth of crystals in the bulk of the glass particles, while in the F12 glass with $\Delta T_p < 0$ the first crystal nuclei will develop on the surface of the glass grains.

Regarding the temperature of the second crystallization peak (T_{p2}), it can be noted that it is not influenced by the glass particle size, since for each glass composition these peaks match at the same temperature in the DSC curves recorded from fragment and powder glass samples.

Concerning T_{gr}, Fig. 4 shows that all glass compositions are locate in the region of the graph corresponding to a predominant volume crystallization mechanism. However, T_{gr} values are very close to the $T_{gr} = 0.58 - 0.60$ interval, which defines the conversion in the mechanism of crystallization, suggesting that in a lesser extent, surface crystallization is also contributing to the devitrification process of these F-phlogopite based glasses. Fig. 4 also displays that T_{gr} slightly increases with fluorine content in fragment samples, which further indicates that increasing the fluorine content in the glass composition slightly increases the degree of surface crystallization.

Therefore, the evaluation of the ΔT_p and T_{gr} parameters suggests that in a subsequent thermal treatment, the volume crystallization mechanism will be predominant in the process of devitrification of these F-phlogopite based glasses. Nevertheless, the increasing fluorine content in the glass composition leads to a variation in the location of the first developed crystals from the internal volume of the glass particle to surface sites.

To verify the preferred crystallization mechanism (surface or volume) by which the crystallization of these F-phlogopite based glasses takes place, samples of glass frit of the different compositions were subjected to a heat treatment at 850°C for 10 minutes. Fig. 5 shows the microstructure of the resulting materials, observed by FESEM. Fig. 5a clearly confirms that the FE glass devitrifies through a preferential volume crystallization mechanism, resulting in a glass-ceramic material composed of tiny small crystals uniformly distributed throughout the whole volume of the material. An additional treatment of FE glass at 850°C for 10 min (Fig. 5b) promotes the development of crystals at the surface of frit particles and small flakes or pseudo-hexagonal crystals with an average size of 2.5 x 0.8 µm are detected by FESEM. EDS analyses collected from these crystals provide an average composition of SiO_2 41.86, Al_2O_3 21.10, MgO 24.51, K_2O 5.67, F_2 5.99 (wt. %), which allows their identification as F-phlogopite phase.

Figs. 5c,d reveals that volume crystallization keep going the preferred devitrification mechanism in the F10 and F12 glasses; however in this case a thermal treatment at 850°C for 10 minutes is enough to promote the growth of crystals on the surface of the glass particle. A crystallization shell is developed, and its depth increases significantly with increasing fluoride content in the glass composition, from 1-3 μm thick in the F10 glass to 20-30 μm thick in the F12 glass. Therefore, it is found that increasing the content of fluoride in the glass composition enhances the extent of surface crystallization.

Regarding the thermal stability of these F-phlogopite glasses, Fig. 6 shows that the values of ΔT_{TS} determined from the fragment samples are in all glasses higher than those for powder samples, indicating that the latter are thermally less stable and therefore show a greater ability to develop crystalline phases in subsequent thermal treatments [44]. Furthermore, for a given glass composition the difference in the values of ΔT_{TS} corresponding to different particle size samples increases with the percentage of fluoride in the composition. The superior ability to devitrify of powdered glass samples were also inferred from Fig. 7, in which the Weinberg, Hruby and Lu-Liu parameters are presented. The values determined from the fragment samples are higher to those determined from DSC curves of powder samples, which support the greater thermal stability of coarse samples.

The glass forming ability (GFA) of these glasses has been evaluated by means of the critical cooling rate calculated from the K_H, K_W and K_{LL} parameters. The values given in Table 3 indicate that the compositions of these glasses result in melts with a high tendency to crystallize on cooling, since in all cases the critical cooling rate is always higher than 120°C/min. This result explains the experimental difficulties encountered for obtaining bulk shape from these F-phlogopite glasses, which have only been obtained as frit by pouring the melt on water, since this ensures that the cooling of the melt is performed at rate higher than the critical cooling rate. Fig. 8 comes to confirm this result, the liquids originated from the melting of the three glass compositions show tendency to crystallize, as evidenced by the presence of exothermic effects in their DSC curves recorded on cooling (Fig. 8a). The occurrence of crystallization effects indicate that the cooling rate applied (50°C/min) is not high enough to prevent crystallization and thereby obtain a completely amorphous material. This result is consistent with the high values of critical cooling rate determined from Weinberg, Hruby and Lu-Liu parameters (Table 3), which are higher than 50°C/min for all the glasses investigated.

It is observed that fluorine increases the tendency to crystallization of these melts on cooling since as the fluorine content of the initial composition is increased, the crystallization peaks in Fig. 8a are more pronounced and located at higher temperatures, varying from a slight

exothermic effect in the FE melt to two well defined high intensity peaks in the F12 liquid. This trend is likely due to the fact that a high content of fluoride ions decreases the melt viscosity, thus increasing the molecular mobility and facilitating the rearrangement of the basic units, resulting in the formation of crystalline phases during cooling [37].

DCS curves in Fig. 8b reflect the typical pattern of a glass with tendency to crystallize during heating. A small endothermic jump corresponds to the glass transition temperature; after that an exothermic effect indicates the existence of at least one crystallization process and finally, endothermic effects due to the formation of liquid phases were observed at higher temperatures. This result suggests that although crystallization has occurred on cooling of the melt, it has not been completed so that a fraction of the resulting material is amorphous after cooling and susceptible to crystallization on a subsequent heating. Fig. 8b denotes that the increases in the fluorine content shifts T_p toward higher temperatures, simultaneously increasing the intensity of the exothermic peak, indicating that fluorine also increases the ability of the residual amorphous phase remained after cooling to devitrify on heating.

Thus, Fig. 8 shows that a higher content of fluorine in the compositions of these F-phlogopite based glasses promotes the crystallization tendency, both on cooling of the melt and during the subsequent heating of the resulting material.

Fig. 9 shows the XRD patterns of the resulting materials after stopping the cooling of the molten glasses to promote the growth of crystalline phases. The cooling of each melt was stopped at the temperature of their corresponding exothermic effect in Fig. 8a, i.e. 1255ºC for FE, 1265ºC for F10 and 1360 º C and 1300 º C for F12 compositions. Fig. 9 evidences yet again the high tendency of these melts to devitrify on cooling. Both the cooling rate in this test (50°C/min), which is in all cases lower than the critical cooling rates collected in Table 3, and the dwell time (30 minutes) at the temperature of treatment makes possible the development of glass-ceramics materials with high crystallisation degree. It is noted the exception of the F12 melt treated on cooling at 1360°C, in which the material resulting is completely amorphous. The proximity to the melting temperature (1450°C) could be related to this result. In all cases, the crystalline phase identified by the peaks of highest intensity is F-phlogopite (PDF 16-0352). The relative intensity of crystallization increases quickly with the fluorine content in the melt composition, so that the glass-ceramic developed from F12 melt presents a higher degree of crystallization. Taking the diffraction peak of greater intensity ($2\theta = 26.78°$), the relative intensities of crystallization for the glass-ceramics derived from FE and F10 compositions are ~ 5% and ~ 64% respectively.

Fig. 10 shows an extension of the XRD pattern of the glass-ceramic material produced by stopping the cooling of the FE melt at 1254°C for 30 min. It can be seen that along with F-phlogopite, forsterite (Mg_2SiO_4, PDF 85-1364) is also devitrified. In this case, F-phlogopite crystallizes in minor extent on cooling of the melt leaving the liquid composition magnesium and silicon ions, which are available for the formation of new crystalline phases.

5. Conclusions

Three F-phlogopite based glasses in the SiO_2-MgO-K_2O-F system were evaluated by DSC to ascertain the effect of fluorine content on their glass forming ability, glass stability and preferential crystallisation mechanism. The results conclude that in the devitrification process of F-phlogopite glasses two crystallization mechanisms coincide, surface and volume. The evaluation of ΔT_p and T_{gr} parameters suggests that in subsequent thermal treatments these glasses preferentially devitrify by a volume crystallization mechanism ($T_{gr}< 0.58$). Although an increase of fluorine content favours the progress of a surface crystallization mechanism, it never reaches the significance of volume crystallization. However, the increasing fluorine content in the glass composition leads to a modification in the location of the first developed crystals from the internal volume of the glass particle to surface sites.

The thermal glass stability (ΔT_{TS}) of these glasses is affected by particle size, so that a glass powder sample (<63 μm) shows a greater ability to crystallize than a fragment sample.

The critical cooling rates of the melts, determined by Weinberg, Hrubÿ and Lu-Liu parameters (K_H, K_W y K_{LL}) are always above 120ºC/min, which explains the experimental difficulty to obtain these glasses in bulk form.

Acknowledgements

The authors would like to acknowledge Mrs. P. Díaz for her technical support in the experimental study. R. Casasola and J.M. Pérez express their gratitude to the Spanish National Research Council (CSIC) for their contract through the JAE Program (JAEPre-08-00456 and JAEDoc-08-00362, respectively), which is co-financed by the European Social Fund. The financial support through the project MAT 2006-05977 is also recognised.

References

[1] Deer WA, Howie RA, Zussman J. An introduction to rock-forming minerals, 2nd ed. London: Pearson Education Ltd.;1996.

[2] Faeghi Nia A. Thermochim Acta 2013;564:1.

[3] Faeghi Nia A. Glass Phys Chem 2014;40:215.

[4] Faeghi-Nia A, Ebadzadeh T. Ceram Int 2012;38:2653.

[5] Ghasemzadeh M, Nemati A. Bull Mater Sci 2012;35:853.

[6] Khalkhali Z, Hamnabard Z, Eftekhari Yekta B, Nasiri M, Khatibi E. J Mater Eng Perform 2013;22:528.

[7] Baik DS, No KS, Chun JS. J Mat Sci 1995;30:1801.

[8] Grossman DG. J Amer Ceram Soc 1972;55:446.

[9] Baik DS, No KS, Chun JS, Cho HY. J Mater Process Technol 1997;67:504.

[10] KhatibZadeha S, Samedanib M, Eftekhari Yektab B, Hasheminiac S. J Mater Process Technol 2008;203:113.

[11] Faeghi-Nia A, Marghussian VK, Taheri-Nassaj E, Pascual MJ, Durán A. J Amer Ceram Soc 2009;92:1514.

[12] Alizadeh P, EftekhariYekta B, Javadi T. Adv Appl Ceram 2010;109:56.

[13] Chyung K, Dawes SB. Mater Sci Eng A, 1993;62:27.

[14] Casasola R, Rincón JMa, Romero M. J Mater Sci 2012;47:553.

[15] Romero M, Rincón JMa, Acosta A. J Amer Ceram Soc 2004;87:819.

[16] Abo-Mosallam HA, Salama SN, Salman SM. Ceram Int 2014;40:8037.

[17] Lendvayova S, Moricova K, Jona E, Uherkova S, Kraxner J, Pavlik V, Durny R, Mojumdar SC. J Therm Anal Calorim 2013;112:1133.

[18] Reben M, Sroda M. J Therm Anal Calorim 2013;113:77.

[19] Heireche MM, Belhadji M, Hakiki NE. J Therm Anal Calorim 2013;114:195.

[20] Sharda S, Sharma S, Sharma P, Sharma V. J Therm Anal Calorim 2014;115:361.

[21] Svoboda R. J Therm Anal Calorim 2014;118:1721.

[22] Thakur RL, Thiagarajan S. Cent Glass Ceram Res Inst Bull 1966;13:33

[23] Donald IW, Metclafe BL, Gerrard LA, Fong SK. J Non-Cryst Solid 2008;354:301. [24] Turnbull D. Contemporary Physics 1969;10:473.

[25] Weinberg MC. Phys Chem Glasses 1994;35:119.

[26] Hrubÿ A. Czech Phys B 1972;22:1187.

[27] Lu ZP, Liu CT. Acta Mater 2002;50:3501.

[28] Lu ZP, Liu CT. Phys Rev Lett 2003;91:115505.

[29] Nascimento MLF, Souza LA, Ferreira EB, Zanotto E. J Non-Cryst Solid 2005;351:3296.

[30] Nascimento MLF, Dantas NO. Mat Lett 2007;61:912.

[31] Davies HA. Phys Chem Glasses 1976;17:159.

[32] James PF. in: Lewis MH (Ed.), Glasses and Glass-Ceramics. London, Chapman and Hall; 1989.

[33] Zanotto ED., J Non-Cryst Solids 1987;89:361.

[34] Zanotto ED, Weinberg MC. Phys Chem Glasses 1989;30:186.

[35] Donald IW, Metclafe BL, Gerrard LA, Fong SK. J Non-Cryst Solid 2006;352:2993.

[36] Velez M, Smith J, Moore RE, Cerâmica 1997;43:180.

[37] Likitvanichkul S, Lacourse WC. J Mat Sci 1995;30:6151.

[38] Casasola R, Pérez JM, Romero M. J Non-Cryst Solids 2013;378:25.

[39] Radonjić LJ, Nikolić LJ. J Eur Ceram Soc 1994;7:11.

[40] Maiti PK, Mallik A, Basumajumdar A, Kundu P. Ceram Int 2010;35:301.

[41] Omar AA, Hamzawy EMA, Farag MM. Ceram Int 2009;36:115.

[42] Stamboulis A, Hill RG, Law RV. J Non-Cryst Solids (2004);333:101.

[43] Brauer DS, Hill RG, O'Donnell MD. Phys Chem Glasses: Eur J Glass Sci Technol B 2012;53:27.

[44] Donald IW, Metclafe BL, Gerrard LA, Fong SK. J Non-Cryst Solid 2008;354:301.